Design of High Efficiency Flyback Converter with Energy Regenerative Snubber

Chih-Sheng Liao and Keyue M. Smedley
Power Electronics Laboratory, Dept. of EECS
University of California, Irvine, CA 92697, USA
smedley@uci.edu

***Abstract*-The Flyback converter is frequently used for multiple outputs and low power application due to its simplicity and both step-up and step-down characteristics. However, the high leakage inductance of the flyback transformer can causes high voltage spike and could damage the main transistor when the switch is turned off. Therefore, a turn-off snubber is needed to limit the peak voltage stress. In this paper, some common snubbers are discussed in comparison with the energy regenerative snubber. The operation of the energy regenerative snubber is analyzed and the design procedures are optimized for energy efficiency followed by experimental verification.**

I. INTRODUCTION

Low component count has been a notable advantage of the Flyback. In this converter, only one magnetic component.is required to perform both the islation and filter functions. One challenge in design the Flyback converter is handling the high leakage inductance of flyback transformer that causes high voltage spike and could damage the main transistor when it is turned off. A variety of turn-off snubbers were reported to limit the rate of rise voltage across the switching device, such as the conventional dissipative RCD snubbers and some non-dissipative snubbers. The RCD snubber is simple, but the power stored in snubber capacitor dissipates on the resistor, thus the efficiency suffers. The LC snubber proposed in [1] achieves lossless operation, but requires an additional inductor that increases the component cost. The energy regenerative snubber developed at UCI Power Electronics Labortory [4] uses the same number of component as RCD yet allows the clamp voltage to be much lower. It can recover leakage energy from snubber capacitor to the dc bus, thus improving energy efficiency.

In Fig.1 (a) a RCD snubber is in parallel with the primary winding. The power stored in the capacitor during turn off period is dissipated on the resistor when switch is turned on. As a result the power loss of dissipative snubbers is significant that cannot meet high efficiency requirement for modern power supply. Fig. 1 (b) shows a non-dissipative LC snubber. It uses combination of diode, inductor and capacitor to transport and store energy without dissipating it. The turn off switching loss can obviously be decreased. Article [3] proposed energy regenerative snubber that has low component count in addition to the advantage of the non-dissipative LC snubber. In this paper, design and optimization of energy regenerative snubber was performed. Engineering design guidelines are provided. An experimental prototype was built to verify the theoretical findings.

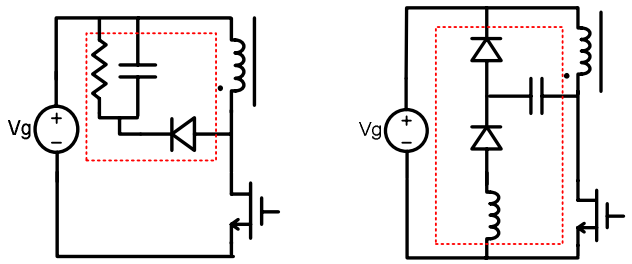

Fig 1. (a) Dissipative RCD snubber
(b) Non-dissipative LC snubber

II. ANAYSIS OF ENERGY REGENERATIVE SNUBBER

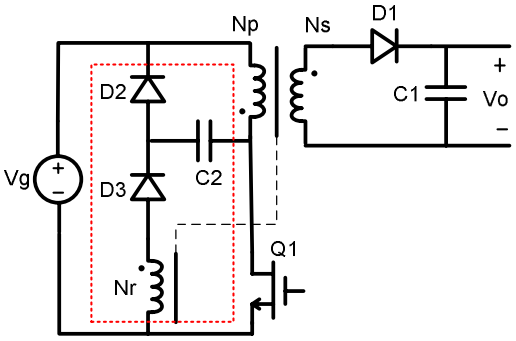

Fig. 2. Flyback with energy regenerative snubber

Table I Devices conduction modes

	$t_0 \sim t_1$	$t_1 \sim t_2$	$t_2 \sim t_3$	$t_3 \sim t_4$
MOSFET	ON	O N	OFF	OFF
Diode 1	OFF	OFF	ON	ON
Diode 2	OFF	OFF	ON	OFF
Diode 3	ON	OFF	OFF	OFF

Fig. 2. shows a flyback converter with energy regenerative snubber. Although only one output is studied, the energy saving principle is applicable to multiple windings. This

978-1-4244-1874-9/08/$25.00 ©2008 IEEE

converter has four switching operating modes as highlighted in Table I. Note that the transformer has three windings with turns ratio Np: Ns: Nr and magnetizing inductance L_m is large compared with the leakage inductance L_{LK}.

In interval t0~t1: When Q_1 is turned on, D_3 conducts and C_2 discharges through Q_1 and reset winding Nr. V_g is applied on L_m and L_{LK}. The equivalent circuit during this interval is shown in Fig.3. (b)

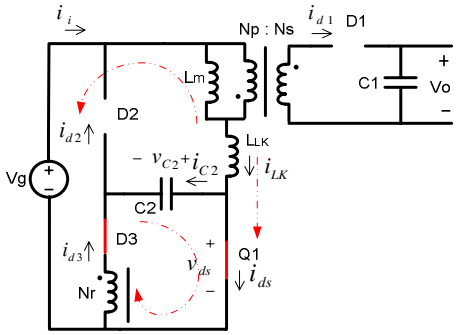

(a)

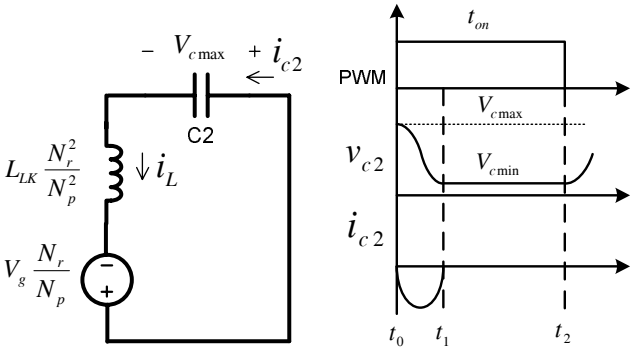

(b) (c)

Fig. 3. (a) Interval t0~t1 sub-circuit
(b) Equivalent circuit of interval t0~t1
(c) Voltage and current waveforms of C_2

From the equivalent circuit, the capacitor voltage and inductor current of this resonant circuit can be expressed as

$$v_{c2}(t) = V_g \frac{N_r}{N_p} - (V_g \frac{N_r}{N_p} - V_{c\max})\cos\omega_0 t \quad (1)$$

$$i_L(t) = \frac{(V_g \frac{N_r}{N_p} - V_{c\max})}{Z_0}\sin\omega_0 t \quad (2)$$

Where angular resonance frequency is

$$\omega_0 = \frac{1}{\frac{N_r}{N_p}\sqrt{L_{LK}C_2}} \quad (3)$$

Characteristic impedance is

$$Z_o = \frac{N_r}{N_p}\sqrt{\frac{L_{LK}}{C_2}} \quad (4)$$

It is easy to see from Fig.3. (c) that $V_{c\ min}$ occurs at half resonant cycle $\omega_0 t = \pi$. Substitute this condition to (1) results following equation.

$$V_{c\min} = 2V_g \frac{N_r}{N_p} - V_{c\max} \quad (5)$$

In interval t1~t2: After t1, D_3 ceases conducting once i_{c2} flows toward reverse direction. L_m is charged by dc bus and the voltage of C_2 remains to be $V_{c\ min}$ until Q_1 is turned off.

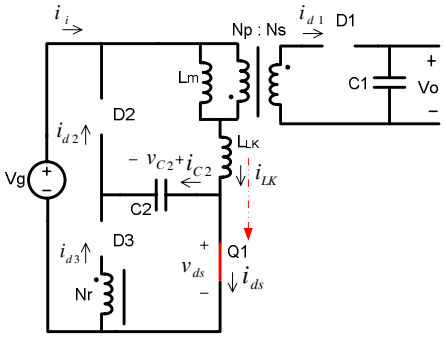

Fig. 4. Interval t1~t2 sub-circuit

In interval t2~t3: Q_1 is turned off and D_2 conducts. The energy stored in L_{LK} transfers to C_2 and the peak voltage stress of switch is limited by the clamp voltage of C_2.
Equations during t2 ~ t3 for this resonant circuit is

$$i_L(t) = i_L\cos\omega_0 t + \frac{V_o\frac{N_p}{N_s} - V_{c\min}}{Z_0}\sin\omega_0 t \quad (6)$$

$$v_c(t) = V_o\frac{N_p}{N_s} - (V_o\frac{N_p}{N_s} - V_{c\min})\cos\omega_0 t + Z_0\cdot i_L\sin\omega_0 t \quad (7)$$

Where i_L in (7) is the magnetizing current I_m. The capacitance of C_2 should be selected to have $V_{c\ min}$ equal V_o*Np/Ns. Substitute those quantities into (6) and (7) yields following relationships.

$$i_L(t) = I_m\cos\omega_0 t \quad (8)$$

$$v_c(t) = V_o\frac{N_p}{N_s} + Z_0\cdot I_m\sin\omega_0 t \quad (9)$$

From (8), the current in leakage inductance drops to zero at $\pi/2$. At this moment, $v_c(t)$ reaches the maximum clamp voltage $V_{c\ max}$.

$$V_{c\max} = V_o\frac{N_p}{N_s} + Z_0\cdot I_m = V_{c\min} + I_m\cdot\sqrt{\frac{L_{LK}}{C_2}} \quad (10)$$

Substitution of (5) and (10) yields

$$V_{c\min} = V_g\frac{N_r}{N_p} - \frac{I_m}{2}\sqrt{\frac{L_{LK}}{C_2}} \quad (11)$$

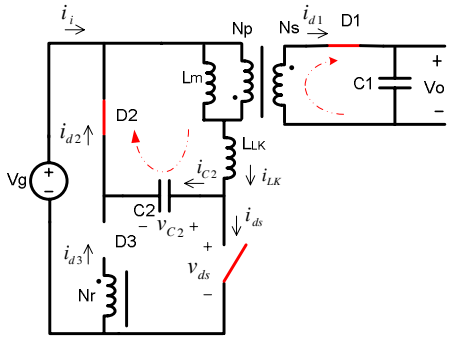

(a)

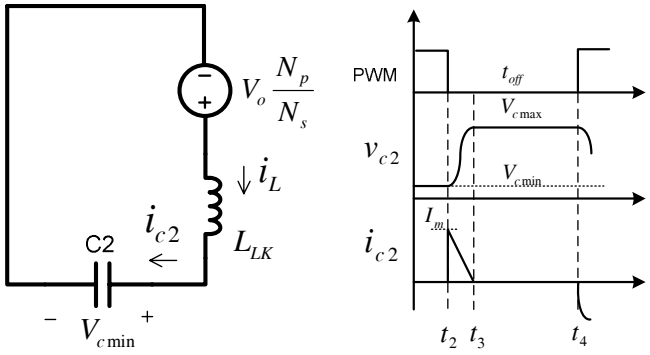

(b) (c)

Fig. 5. (a) Interval t2~t3 sub-circuit
(b) Equivalent circuit of interval t2~t3
(c) Voltage and current waveforms of C_2

In interval t3~t4: After t3, the current in the leakage inductance decreases to zero until the next turn-on state. The whole processes of four intervals repeat in each cycle.
The analysis shows that the snubber capacitor C_2 and reset winding Nr are two crucial parameters to the operation of circuit. The design procedures will be depicted in the next section.

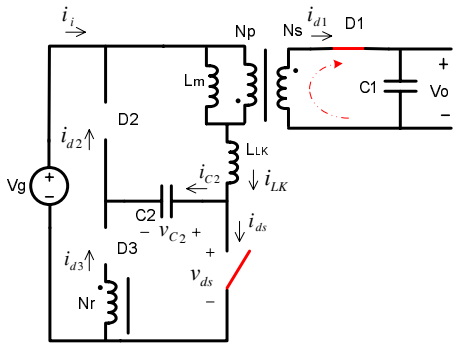

Fig. 6. Interval t3~t4 sub-circuit

III. DESIGN PROCEDURES

Turns of reset winding: When the transistor is on, diode D_2 and D_1 are reverse biased. Diode D_3 is on until V_{c2} drops to the reflected input voltage, V_g*Nr/Np. During the transistor-on period, V_{c2} is approximately equal to the voltage of the clamp winding Nr.

$$V_{C2} = \frac{N_r}{N_p} \cdot V_g \tag{12}$$

Voltage V_{c2} must be greater than the reflected output voltage so that D_1 will not be reverse biased during the transistor-off period, otherwise the energy stored in L_m will be totally transferred to the capacitor instead of the output winding. Therefore,

$$V_{C2} > \frac{V_o \cdot N_p}{N_s} \tag{13}$$

Substituting (12) into (13), the turns of clamp winding can be determined by the inequality

$$N_r > \frac{V_o \cdot N_p^2}{V_g \cdot N_s} \tag{14}$$

Choice of the clamp capacitance: To meet the requirement of (13), the minimum voltage level of C_2, $V_{c\,min}$, in (11) needs to be greater than V_o*Np/Ns. Solving the inequality, the capacitance is given as follows

$$C_2 \geq \frac{I_m^2 \cdot L_{LK}}{4 \cdot V_o^2 \cdot (\frac{N_r}{N_s}\frac{1-D}{D} - \frac{N_p}{N_s})^2} \tag{15}$$

Timing limitation: It is required that during transistor-on time the half cycle of the LC resonant should be completed. This gives a constraint on the maximum value of clamp capacitance.

$$C_2 < \left(\frac{T_{on} N_p}{\pi N_r}\right)^2 \frac{1}{L_{LK}} \tag{16}$$

IV. SIMULATION AND EXPERIMENTAL RESULTS

PSIM simulation program was used to emulate the performance and a prototype of flyback converter was built as shown in Fig. 7.

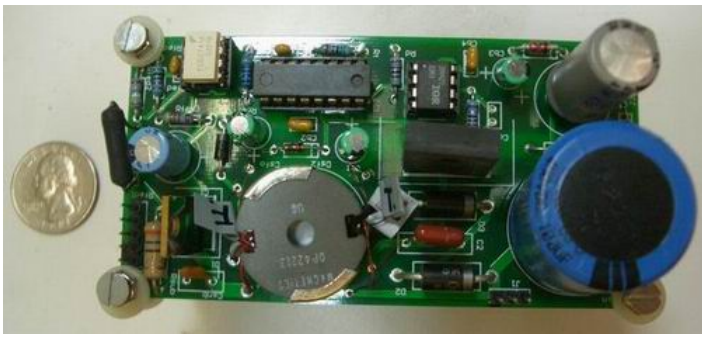

Fig. 7. 50W prototype of flyback with energy regenerative snubber

The experiment conditions are:

Input voltage range:	300V ~ 400V
Output voltage:	24V
Maximum output power:	50W
Switching frequency:	100kHz

The figures shown below are in the same time scale. It can be observed from Fig. 8 ~ Fig. 13. that t0~t1 is the period when clamp capacitor C_2 discharges through Q_1 and Nr while D_3, C_2 and L_{LK} resonant . The current of C_2 is a half sine wave and the voltage of C_2 is a half cosine wave. Between t2 to t3, the snubber is in clamp mode. The energy stored in leakage inductance is transferred to C_2 during this time. The leakage current dropped to zero quickly. In Fig. 9, a gradual drain-to-source voltage-rise is visible when the MOSFET is turned off. Fig. 9, Fig. 11 and Fig. 13 are experimental waveforms which are in accordance with the theoretical analysis and simulation.

For efficiency study, a comparison is made with the traditional RCD method and the LC lossless snuber method. The power efficiencies were measured on the same flyback prototype with different snubbers. The designed parameters of RCD, non-dissipative LC and energy regenerative snubber are given in Table II, Table III and Table IV, respectively. The curves of efficiency of three different snubbers under the same voltage stress are shown in Fig.13. It is observed that the overall efficiency of energy regenerative snubber is about 8% higher than that of RCD and about 2 % higher than that of the non-dissipative LC snubber,

Table II The parameters of flyback with RCD snubber

Np	Ns	L_m	L_{LK}	$R_{snubber}$	$C_{snubber}$
74	11	2.33mH	36.3uH	20kohm	100nF

Table III The parameters of flyback with Non-dissipative LC snubber

Np	Ns	L_m	L_{LK}	$L_{snubber}$	$C_{snubber}$
74	11	2.33mH	36.3uH	4.5uH	1nF

Table IV The parameters of flyback with energy regenerative snubber

Np	Ns	Nr	L_m	L_{LK}	$C_{snubber}$
74	11	48	2.33mH	36.3uH	10nF

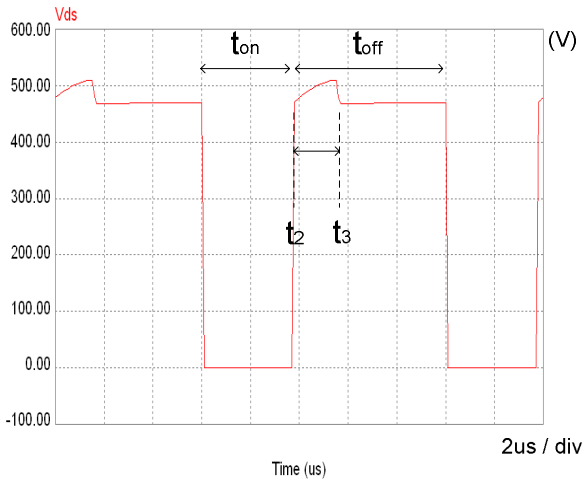

Fig. 8. Simulated voltage waveform of transistor

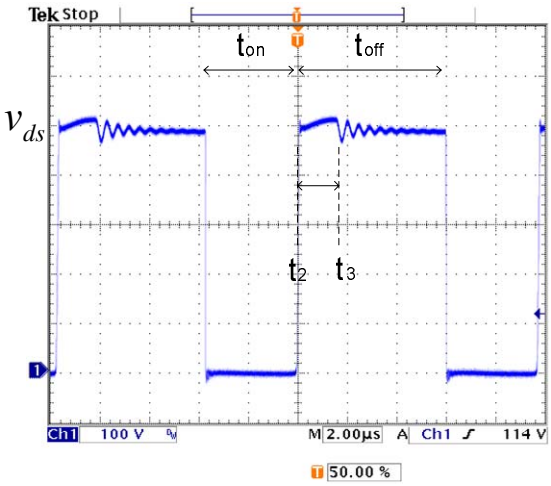

Fig. 9. Experimental voltage waveform of transistor

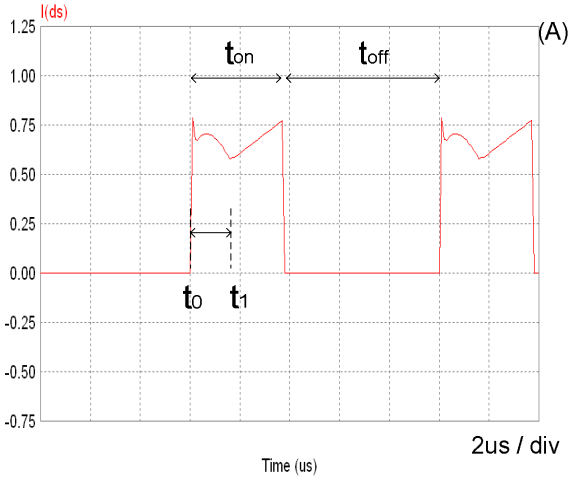

Fig. 10. Simulated current waveform of transistor

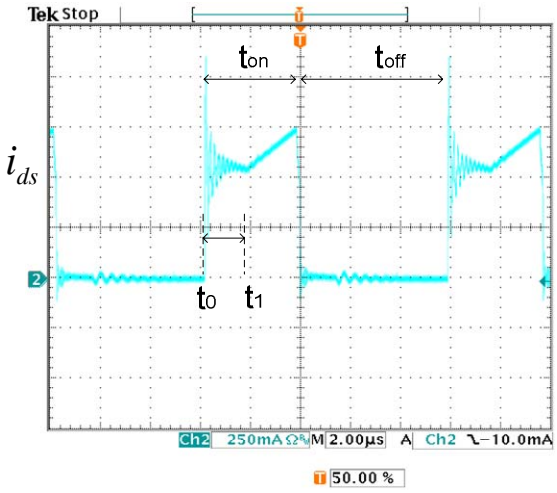

Fig. 11. Experimental current waveform of transistor

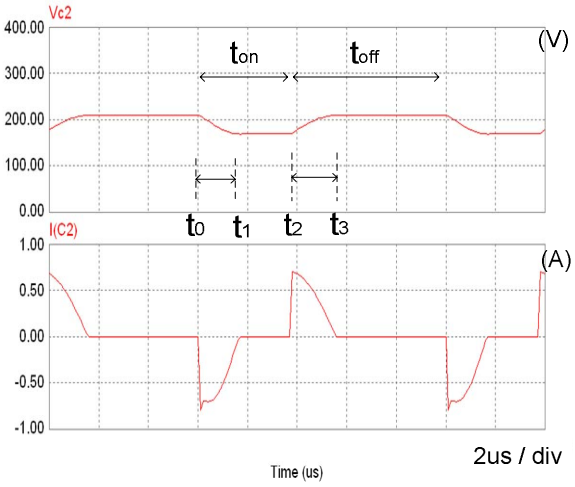

Fig. 12. Simulated voltage and current waveforms of C_2

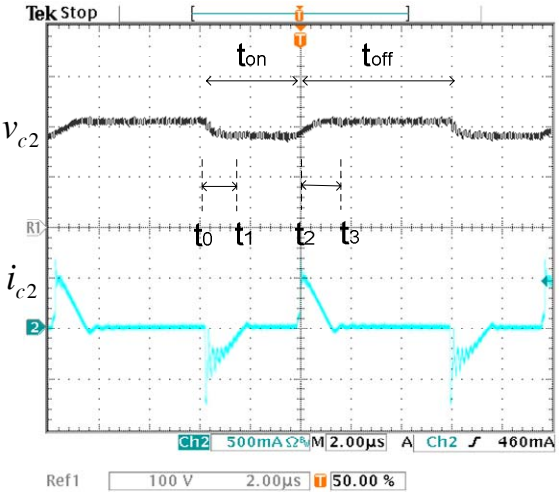

Fig. 13. Experimental voltage and current waveforms of C_2

V. CONCLUSION

With an RCD snubber, the voltage stress of the switch and the power dissipation of the snubber are a trade-off. They are determined by the value of snubber resistor. The high power dissipation has long been its drawback. The non-dissipative LC snubber can significantly reduce the loss of snubber circuit. However, an extra inductor for the snubber increases the cost and makes design more complicated. In comparison, the voltage stress of the energy regenerative snubber is set by the turns of reset winding Nr without sacrificing efficiency. Moreover, the clamp winding shares the same core with the transformer, which is cost effective and easier to design. The experimental efficiency in Fig. 14. shows that under the same voltage stress the efficiency of energy regenerative snubber has 8% improvement in average over RCD snubber and 2% improvement over nondispative LC snubber.

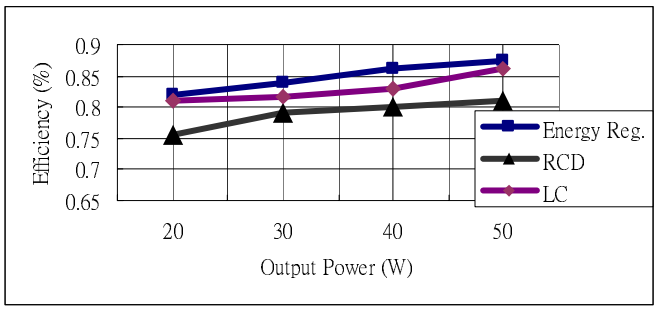

Fig. 14. Experimental efficiency measured with RCD, non-dissipative snubber and energy regenerative snubber.

REFERENCES

[1] Moshe Domb, Richard Redl, and Nathan O Sokal "Non-dissipative Turn Off Snubber Alleviates Switching Power Dissipation, Second-Breakdown Stress and VCE Overshoot: Analysis, Design Procedure and Experimental Verification".

[2] Moshe Domb, Richard Redl, and Nathan O Sokal "Non-dissipative Turn-Off Snubber in a Forward Converter: Analysis, Design Procedure, and Experimental Verification" PCI Proceeding 1985.

[3] K. M. Smith, Chuanwen Ji, and K. M. Smedley, "Energy regenerative clamp for flyback Converter", UCI, invention disclosure, Sept. 1998.

[4] Chuanwen Ji, K. Mark Smith, Jr., and Keyue M. Smedley "Cross Regulation in Flyback Converters: Analytic Model and Solution" *IEEE Trans. On Power Electronics, Vol. 16, No.2, March 2001.*

[5] Alenka Hren, Joze Korelic, and Miro Milanovic "RC-RCD Clamp Circuit for Ringing Losses Reduction in a Flyback Converter" *IEEE Trans. On Circuits and systems—II:Express Briefs. Vol. 53. No. 5 May 2006.*

[6] Tsu-Hua Ai, "A Novel Integrated Non-dissipative Snubber for Flyback Converter"

[7] Robert W. Ericson, and Dragon Maksimovic, "*Fundamentals of Power Electronics" Second Edition.*

[8] N. Mohan, T. M. Undeland, and W. P. Robbins, "*Power Electronics; Converter, Applications and Design" Third Edition.*

[9] "*Snubber Circuits Suppress Voltage Transient Spikes in Multiple Output DC-DC Flyback Converter Power Supplies*", Application note 848, http://www.maxim-ic.com/appnotes.cfm/appnote_number/848